Hindawi
Geofluids
Volume 2022, Article ID 9094890, 16 pages
https://doi.org/10.1155/2022/9094890

Research Article

New Methods for Predicting Strain Demand of Arctic Gas Pipelines across Permafrost under Frost Heave Displacement

Xinze Li,[1,2,3] **Qingbai Wu**,[1,2] **and Huijun Jin**[1,2,4]

[1]*State Key Laboratory of Frozen Soils Engineering, Northwest Institute of Eco-Environment and Resources, Chinese Academy of Sciences, Lanzhou 730000, China*
[2]*School of Resources and Environment, University of Chinese Academy of Sciences, Beijing 100049, China*
[3]*Department of Chemical and Material Engineering, University of Alberta, Edmonton, AB, Canada T6G 1H9*
[4]*Northeast-China Observatory and Research-Station of Permafrost Geo-Environment (Ministry of Education), Institute of Cold-Regions Science and Engineering, School of Civil Engineering, Northeast Forestry University, Harbin 150040, China*

Correspondence should be addressed to Xinze Li; xinze4@ualberta.ca

Received 17 December 2021; Revised 30 January 2022; Accepted 28 February 2022; Published 25 March 2022

Academic Editor: Qingzhi Wang

With increasing gas resource development in the Arctic region, gas pipeline installations in permafrost regions are becoming important. Frost heave of pipeline foundation soils may occur when a chilled gas pipeline passes through unfrozen areas with frost-susceptible soils. The stress and strain behaviors caused by the differential frost heave will directly affect the safety of the pipeline. A nonlinear finite element model (FEM) computing the mechanical responses of the buried gas pipeline subjected to frost heave load was established and successfully validated with the results of a large-scale indoor pipe-soil interaction experiment carried out in Caen in France. Utilizing C# language and object-oriented visual programming techniques, a new customized parametric strain calculation software was developed. The effects of pipe diameter, pipe wall thickness, pipe internal pressure, and peak soil resistance on the longitudinal strain of X60, X70, and X80 steel pipes have been investigated quantitatively. For the first time, a fitting semiempirical equation and trained backpropagation neural network (BPNN) for predicting pipeline strain demand subjected to frost heave load were proposed based on 2688 groups of FEM results. The comparison results have proved their high accuracy and lower running time cost. The proposed new methods can be applied in the strain-based pipeline design and safety evaluation of pipelines in service. It is in the hope of supplementing existing theory and identifying new approaches for arctic gas pipeline installations.

1. Introduction

Arctic regions are rich in natural gas resources. Gas exploration, development, and pipeline construction thus have received increasingly more attention. For the sake of security, environment, and economics, a proposed buried, chilled pipeline system is preferred to prevent the thawing of permafrost. It is unavoidable that the arctic gas pipeline will cross continuous and discontinuous permafrost regions and seasonal frost regions from north to south. Li et al. [1] established a geothermal model of the interactions between pipeline and permafrost. The thermal effect of pipelines with 5°C, -1°C, and -5°C settings of gas flow on the freezing and thawing of soil around the pipeline were investigated. In terms of thermal stability around the pipeline, it is advised that a transporting temperature of gas flow approaching -1°C should be adopted in continuous permafrost regions all year round which causes only little disturbance to the permafrost environment. In the discontinuous permafrost regions, the pipeline could be operated under above-freezing temperatures in the warm season with the station discharge temperature approximating to the ambient air temperatures, but the discharge temperature must be maintained approaching -1°C throughout the cold season. In the seasonal frost regions, the cold (-1°C) and chilled (-5°C) pipeline may cause frost heave; therefore, the pipeline should run at positive temperature without extra temperature cooling control. The operation of gas-to-gas heat exchangers

combined with aerial gas coolers at compressor station locations is considered a feasible method of controlling the gas temperature in the pipeline. Some experience and lessons could be learned from gas pipelines operating in northwest Siberia. Without sufficient cooling after compression, a result of warm gas transmission (invariably well above 0°C) leads to the thaw settlement of pipeline foundation soils and a loss of soil loading-bearing capacity [2].

The frost heave would be anticipated when a chilled pipeline passes through discontinuous permafrost regions with alternating pipeline segments in frozen and unfrozen soils. The water around the pipe moves and freezes near the pipe, and the formation of ice lenses in the soils could occur [3, 4]. These ice lenses become sufficiently thick to vertically displace the pipeline upwards [5, 6]. The differential frost heave hazards could potentially induce excessive stress and strain on pipe resulting in pipeline deformation, upheaval buckling, and even rupture which seriously threaten the structural integrity and long-term safe operation of the pipeline [7]. There are examples such as frost heaving and deformation of the buried Norman Wells Pipeline and Golmud-Lhasa Product Oil Pipeline [8, 9]. Numerous arctic gas pipelines through the interior of Alaska and then along the Alaska Highway and northern Alberta were proposed and studied since the early 1970s. Most notable are Alaska Natural Gas Transportation System (ANGTS), Alaska Pipeline Project (APP), Alaska Stand Alone Pipeline (ASAP), Denali Pipeline Project (Denali), Mackenzie Gas Project (MGP), and Alaska LNG Project [10]. However, restricted by technology, gas economy/markets, environmental protection, geopolitics, and many other factors, these pipelines have not entered the substantive construction stage. Therefore, the engineering practice experience of buried, chilled gas pipelines in permafrost regions is still very limited, at least in North America, challenging the safe construction and operation and long-term serviceability of gas lines. A chilled pipeline passing through discontinuous permafrost regions is particularly exposed to the risk of deformations [11].

To address these potential large ground movements due to frost heave or thaw settlement, the high-level principle of limit state design was first proposed in a nonmandatory Annex C of CSA Z662 [12]. Afterward, these principles were used to develop an alternative design methodology called strain-based design (SBD). This approach is particularly applicable in displacement-controlled load conditions where the strains gradually accumulate over time, such as associated with frost heave or thaw settlement. In the SBD process, if the design strain/strain demand is less than allowable strain/factored strain capacity, then no changes or further design investigation is required for the pipe segment. If design strain exceeds allowable strain, then the pipe segment is designated as an "SBD segment," and mitigation measures such as heavier wall pipe and large strain steel pipe would be adopted. The engineering processes and models used to determine both the design strain and strain capacity are critical in the application of SBD [13]. Adequate pipeline strain capacity to resist the effects of frost heave is an important design consideration. The strain capacity is dependent on pipe tensile and compressive properties. The Norman Wells Pipeline, which came into operation in the mid-1980s across permafrost terrain in North America, adopted the SBD method with a 0.5% limit on the maximum tensile strain and a 0.75% limit on the maximum compressive strain [14]. On the Mackenzie Gas Project (MGP), a strain criteria basis was developed with material specification, line pipe, full-scale testing, and construction to ensure the required strain capacity can be achieved in practice [10].

The nonlinear finite element model (FEM) has been widely applied in the strain demand analysis of buried pipelines subjected to environmental loads. Lots of scholars have studied the strain-stress behaviors of pipelines induced by differential deformation, both experimentally and theoretically. Liu et al. [15] established a mathematical model based on the nonlinear FEM for the X80 steel pipeline crossing an active fault. The influencing factors of pipe diameter, wall thickness, soil rigidity, and crossing angle on the maximum compressive strain were analyzed. And a regression equation was proposed for calculating pipeline strain based on the FEM data. Zheng et al. [16] studied the strain response of the X80 steel pipeline under the effect of strike-slip fault through the nonlinear FEM method. In the model, the pipeline was simulated by the shell elements, and the soil constraints were simulated using the nonlinear spring elements. An artificial neural network was proposed for calculating the strain of the X80 steel pipeline based on the FEM results. Taking the Sino-Russian Crude Oil Pipeline as a prototype, Xia [17] established a FEM calculating the strain responses of X65 steel pipe under thawing settlement load parametrically. The effects of pipe wall thickness, pipe internal pressure, and temperature difference on pipe strain demand have been analyzed. A support vector machine based on a machine learning model was furtherly trained via FEM data to predict strain demand. The company TransCanada has developed a fully integrated model package for arctic pipeline design which consists of three programs: Tempflo, TQUEST, and PIPLIN [18]. They have been used and validated over the last 40 years. The PIPLIN considers several nonlinear aspects of pipeline behavior, including pipe yield, large displacement effects, and nonlinear soil spring.

At present, there are a few regression equations and machine learning models proposed for calculating the strain demand of pipe crossing active faults or thawing zones. The research mainly focuses on X80 or X65 steel grade with the objective of safety assessment of pipeline in service, which provides limited guidance for the new pipelines. With gas resource development in the Arctic region, pipeline installations in permafrost regions such as Alaska LNG Project are brought into a schedule. Strain demand prediction of pipelines subjected to frost heave displacement is of interest to engineers in the context of strain-based design. Numerical simulation is the main method to study the response of the buried pipeline. Although models exist to analyze this problem, these models are quite complex. The pipeline designers who do not master the skill of establishing FEM will have difficulties in pipeline strain calculation.

The main purpose of the paper is to quickly compute the strain demand of the buried pipeline subjected to frost heave

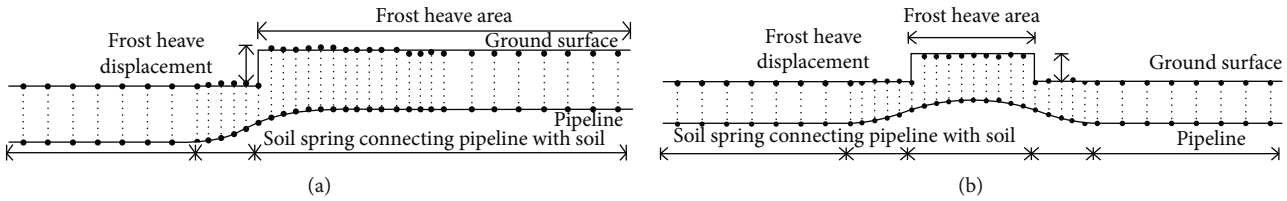

Figure 1: Schematic diagram for buried pipeline subjected to differential frost heave: (a) semi-infinite length model and (b) finite length model.

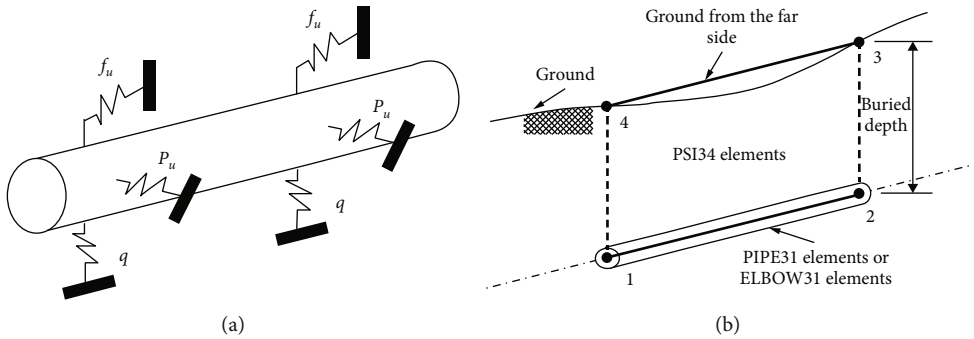

Figure 2: Soil springs simulating soil constraints on pipe: (a) nonlinear soil springs in axial, lateral, and vertical directions and (b) PSI34 elements for pipe-soil interaction.

load with high accuracy and lower running time cost. The objective is to regress the semiempirical equations and to establish a backpropagation neural network (BPNN) prediction model based on a complete package of results from the 2688 individual FEM simulations. Although the approaches used (e.g., finite element and neural network) are well-established ones, the contribution of this work is to present a fitting semiempirical equation and trained network for calculating pipe strain demand subjected to frost heave load for the first time. A new customized parametric strain calculation software for the pipeline was also developed based on ABAQUS utilizing C# language and object-oriented visual programming techniques. This work is meaningful and it is in the hope of providing references for new long-distance gas pipeline development in the Arctic region.

2. Finite Element Model and Developed Software

2.1. Establishment of FEM. The nonlinear finite element code package ABAQUS was used to establish FEMs for pipeline strain calculation under frost heave displacement load. The schematic diagram for semi-infinite length model and finite length model are shown in Figure 1. Semi-infinite length model means that the ground on both sides of the ground dislocation area remains stable for a long enough length. It is not necessary to establish entire pipe segments in modeling, and only half of the pipeline is required. This kind of model applies to the longer heave span length. The finite length model considers the ground displacement that occurs within a certain range. In this case, the soil constraints at both sides of the ground dislocation area must be considered at the same time, and the entire pipeline needs to be established in modeling. This kind of model applies to the short heave span length. In discontinuous permafrost regions, the length of a single frozen or unfrozen segment could range from several meters to kilometers depending primarily on variations in surface conditions. The models consider multiple nonlinearities such as pipe material, pipe-soil interaction, and large geometric deformation, which could accurately describe the stress-strain response of pipelines under frost heave displacement load.

The stress-strain equation proposed by Ramberg and Osgood is a classical model to describe the stress-strain relationship of elastoplastic materials. It is often used to describe the test curves including the Round-House stress-strain curves [19]. The Ramberg-Osgood constitutive equation can well simulate the stress-strain curve of the actual pipe with the yield strain within 4%. Therefore, the Ramberg-Osgood model was selected to describe the actual constitutive relationship of the pipeline. The Ramberg-Osgood model considers the total strain as the sum of elastic strain and plastic strain, and its mathematical expression is shown as follows:

$$\varepsilon = \frac{\sigma_s}{E}\left[\frac{\sigma}{\sigma_s} + \alpha\left(\frac{\sigma}{\sigma_s}\right)^N\right], \quad (1)$$

where ε is the real strain, σ is the axial tensile stress (MPa), E is the elasticity modulus (MPa), σ_s is the yield stress (MPa), and α and N are factors of Ramberg-Osgood. For X80 steel pipeline, $\alpha = 0.86$, $N = 28$, and $\sigma_s = 552$ MPa.

The nonlinear soil springs in axial, lateral, and vertical directions proposed by the American Lifetime Alliance (ALA) were used to simulate soil constraints on the pipe [20]. The soil spring parameters f_u, p_u, and $q_u(q_d)$ represent

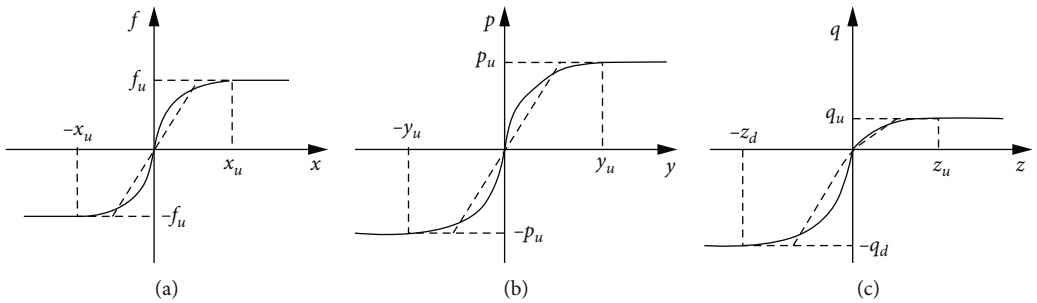

Figure 3: Force-displacement relationships for nonlinear soil springs. (a) axial, (b) transverse lateral, and (c) transverse vertical.

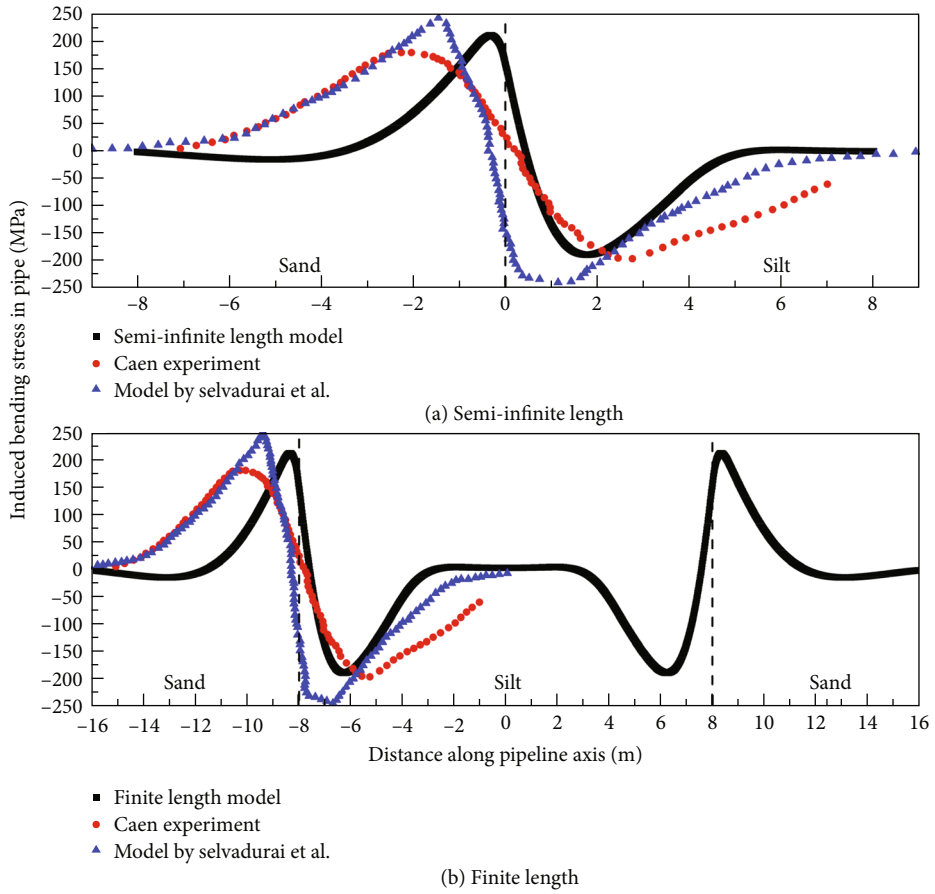

Figure 4: Comparison results of bending stresses in the pipeline subjected to differential frost heave between Caen experiment in France, computational estimates by Selvadurai et al., and differential frost heave models in this paper: (a) semi-infinite length model and (b) finite length model.

the maximum soil resistance forces per unit length of pipes in the axial, lateral, and vertical directions (Figure 2(a)). And x_u, y_u, $z_u(z_d)$ represent the yield displacements, respectively (Figure 3). The values of these parameters can be calculated-by the equations suggested by the ALA-ASCE guideline.

The nonlinear soil springs can be realized by the three-dimensional 4-node pipe-soil interaction elements (PSI34) developed by ABAQUS. PSI34 elements, as shown in Figure 2(b), are composed of four nodes: the top two nodes are connected to the ground surface (node 3 and node 4) reflecting the ground movement and the displacement, and the other two nodes (node 1 and node 2) at the bottom are connected to the pipe elements. The PSI34 elements are connected with the ground surface and pipeline elements at the same time to avoid the meshing of soil in the studying area. The interaction between the pipe and soil is expressed by the nonlinear element stiffness.

The beam elements were used to simulate the structure dominated by longitudinal stress, whose dimension in the axial direction is larger than that of the other two directions. Both PIPE31 elements and ELBOW31 elements belong to beam elements. Take the finite length model for example.

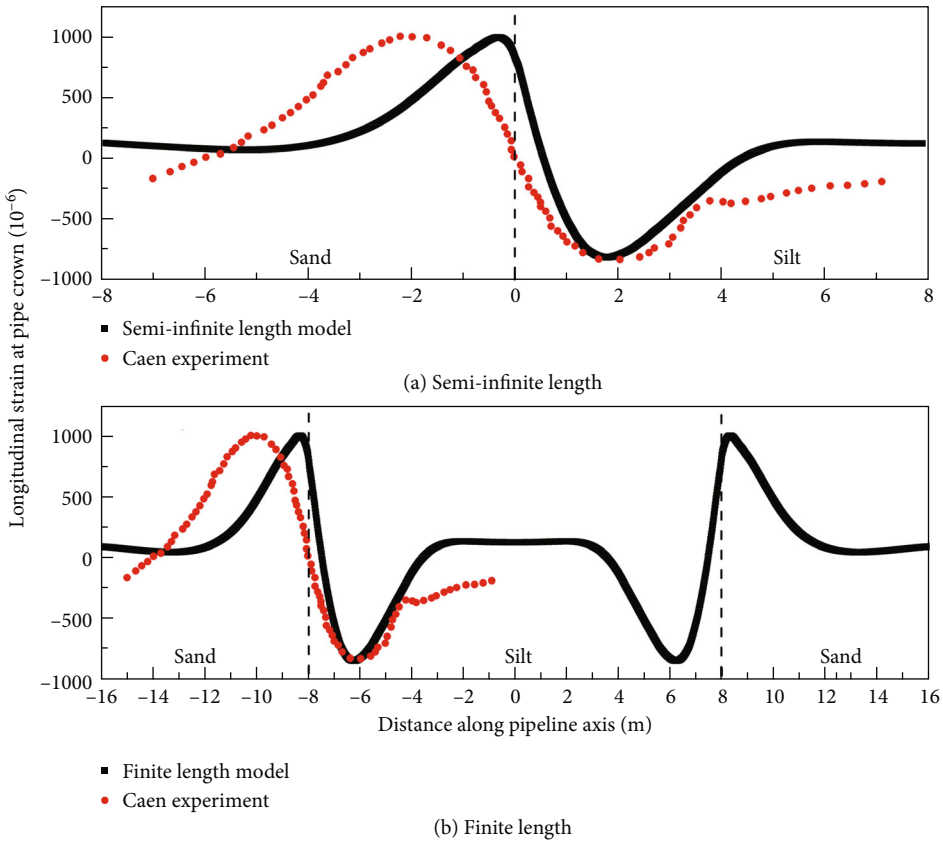

Figure 5: Comparison results of longitudinal strains at pipe crown subjected to differential frost heave between Caen experiment in France and differential frost heave models in this paper: (a) semi-infinite length model and (b) finite length model.

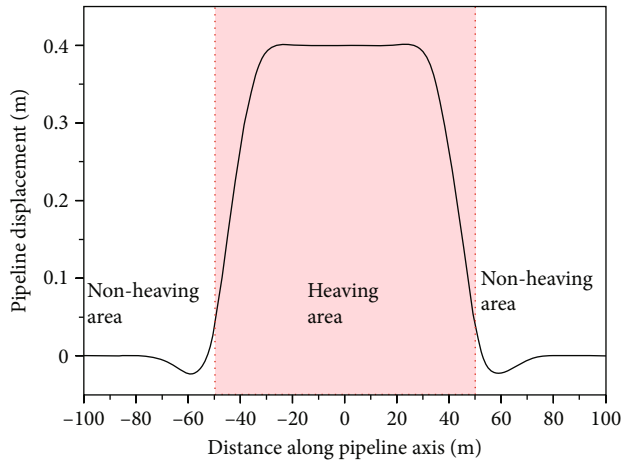

Figure 6: Pipe vertical displacements under frost heave displacement of 0.4 m based on finite length frost heave model.

PIPE31 elements were utilized for the discretization of pipes far away from the heaving area. A coarse mesh with element size of 1 m was set. ELBOW31 elements were utilized to model the pipes near and in the heaving area. A fine mesh with element size of 0.1 m was set, as large pipe stress appears in these pipe segments. By default, the ELBOW31 elements have 20 integral points in the loop direction and 5 integral points in the radial direction, which can obtain the mechanical response of different positions of the pipeline. The ELBOW31 elements can describe the elliptic deformation of cross-sections, resulting in more accurate solutions with less computational cost. So ELBOW31 elements can consider pipe section deformation more accurately compared with the common PIPE31 elements.

Above the pipe, a total of 4001 soil nodes were corresponding to the nodes of PIPE31 elements and ELBOW31 elements on the pipe. The fixed boundary constraints were set at both ends. The length of the pipe model was not a constant value. It was determined by multiple trials based on the criteria that the boundary constraints at both ends do not influence the pipe strain to eliminate boundary effects.

2.2. Model Validation. One famous pipeline-soil interaction experiment was conducted at Le Center de Geomorphologie at Caen, France, by a France-Canada joint team during 1982-1989 and 1990-1993. The Caen frost heave experiment was designed to investigate the thermal and mechanical effects on a buried pipeline crossing a transition between two types of frost-susceptible soils by creating a sharp contrast in the frost susceptibility of soils in the test. A pipeline with a length of 16 m, a diameter of 273 mm, and a wall thickness of 7 mm was buried at 0.33 m depth. The deformation of the pipe carrying gas at -5 to -2°C has been determined by 22 pairs of electrical resistance strain gauges attached to the pipe. The pipeline used in the experiment was made of L245(B) steel

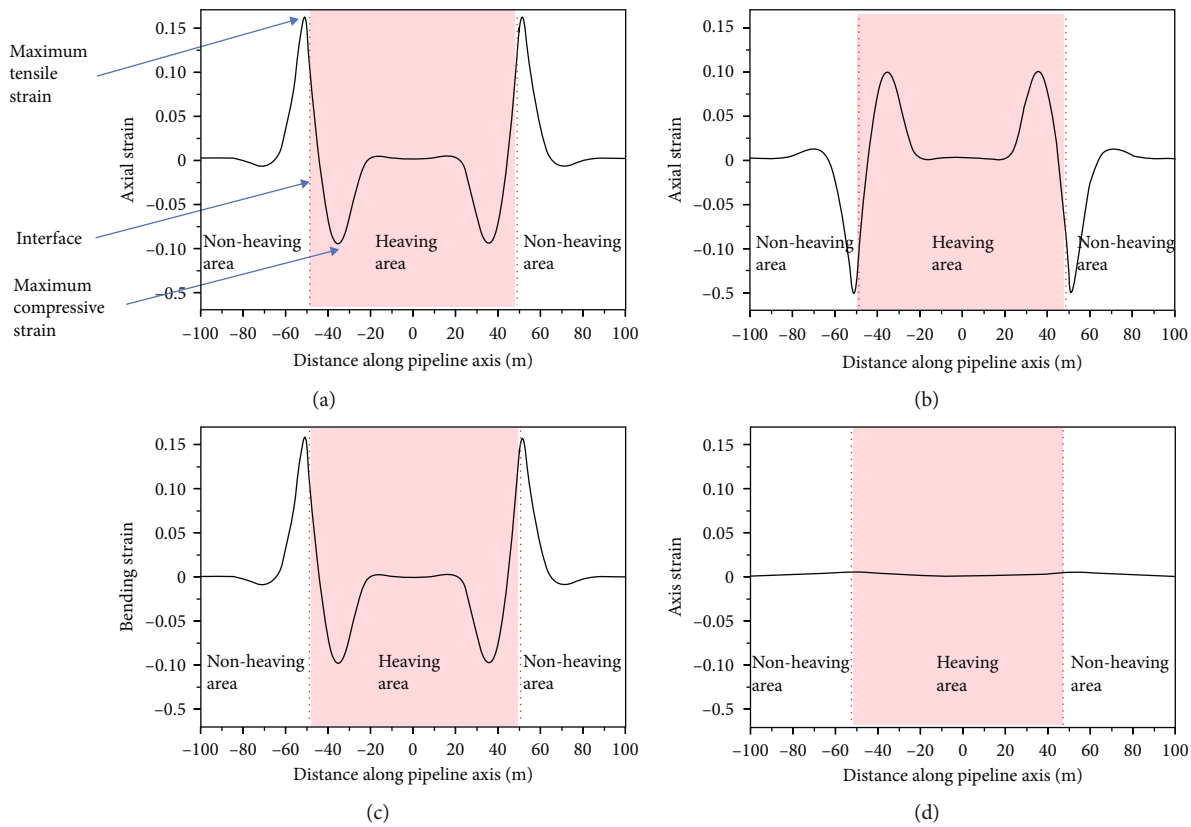

Figure 7: Pipe strain distributions under frost heave displacement of 0.4 m based on finite length frost heave model: (a) axial strain at pipe crown, (b) axial strain at pipe invert, (c) bending strain, and (d) axis strain.

pipe with Young's modulus 200 GPa and Poisson's ratio of 0.3. More complete descriptions of this experiment are given by Williams et al. [21]. Afterward, Selvadurai et al. [22, 23] established three-dimensional computational modeling of the interaction between a buried pipeline and a soil area. The numerical model was also used to develop estimates for pipeline behavior observed in the Caen experiment. These experimental results and computational estimates could be used to validate the FEM established in this paper.

Figure 4 illustrates the comparison results of bending stresses in the pipeline induced by differential frost heave between Caen experiment in France, computational estimates by Selvadurai et al., and semi-infinite length and finite length differential frost heave models in this paper. The pipe displacement subjected to frost heave was set as an experimental result of 0.2 m. The variation trend is similar in the distribution of bending stress in the pipeline. The peak of bending stresses is presented in the vicinity of the interface. The results of the semi-infinite length model and finite length model are almost the same. The relative errors between Caen experimental results and semi-infinite length and finite length models for maximum and minimum bending stresses are 17.2% and 4.1%, respectively.

Figure 5 shows the comparison results of longitudinal strains at pipe crown subjected to differential frost heave between Caen experiment in France and semi-infinite length and finite length differential frost heave models in this paper. The pipe displacement subjected to frost heave was set as an experimental result of 0.1 m. Here again, good agreement is obtained between the experimental results and computational estimates in this paper. The results of the semi-infinite length model and finite length model are almost the same. The relative errors between Caen experimental results and semi-infinite length and finite length models for maximum and minimum strains are 0.8% and 2.3%, respectively. The following reasons can induce the relative error: (i) stress-strain curve of pipeline, (ii) resistance of soil springs, and (iii) physical and mechanical properties of silty clay and sand.

2.3. Distribution Laws of Pipeline Strain. The finite length frost heave model is used to demonstrate the distribution laws of pipeline strain under frost heave displacement. A proposed arctic gas pipeline in Alaska is adopted as a prototype for the investigation. The pipe diameter and pipe wall thickness are 1067 mm and 17.2 mm, respectively. Young's modulus of the X80 pipeline is 207 GPa. The heave span length is 100 m. A fine mesh with element length of 0.1 m was utilized for the middle section where heaving areas were located to obtain the accurate mechanical response of pipe [24]. Meanwhile, a coarse mesh with element size of 1 m was used for pipe segments at the two sides. The variation curve of the vertical displacement of the pipeline along the length of the pipeline is shown in Figure 6. The maximum vertical displacement of the pipeline occurs in the middle of the pipe section, and the maximum vertical displacement

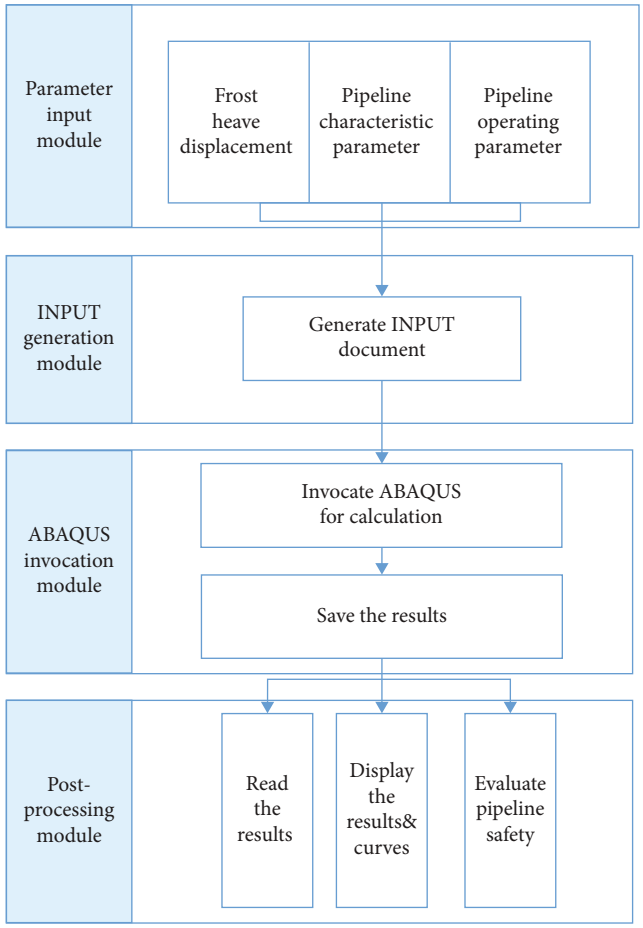

Figure 8: Overall architecture of a customized parametric strain calculation software developed based on ABAQUS.

is 0.4 m. The pipe strain distributions along the length of the pipeline determined via the finite length frost heave model are shown in Figure 7. Take axial strain at pipe crown as an example, the maximum tensile strain generally occurs on the nonheaving side of the frozen-unfrozen interface. The maximum compressive strain also occurs in the vicinity of the transition area and is located in the heaving area. The axial strain direction at the pipe invert is opposite to the strain direction at the pipe crown. Figures 7(c) and 7(d) show the distribution laws of bending strain and axis strain of pipeline. It can be seen that due to the frost heave displacement, the pipe has a large bending moment near the interface, and the bending strain in the axial center of the pipeline is approximately zero. At the same time, the pipe has a certain elongation, forming axis strain in the heaving area.

2.4. Customized Parametric Strain Calculation Software Development. To quickly and conveniently compute the pipeline strain under frost heave displacement load and evaluate the safety status of the pipelines in the permafrost regions, a new customized parametric strain calculation software for the pipeline was developed. It was based on ABAQUS utilizing C# language and object-oriented visual programming techniques. The software mainly includes four modules: parameter input module, INPUT generation module, ABAQUS invocation module, and postprocessing module (Figure 8). The INPUT programming language and macrotechnology were used to organize and manage the commands of ABAQUS, realizing the parameter input, load application, solution, and display of the results. ABAQUS would be invoked in the background for calculation. After the analysis is completed, the design strain curve and allowable tensile and compressive strain curves would be displayed in one figure for comparison.

3. Analysis of Sensitivity Parameters on Pipe Strain Demand

3.1. Sensitivity Parameter Range. To establish the advanced model to predict the strain demand, the first step is to find out the key influencing parameters on the longitudinal strain. Therefore, parametric analysis was performed to analyze the influence of various factors on the pipeline axial strain. A reasonable range of sensitivity parameters (Table 1) was given based on the standard ASME B31.8 (Gas Transmission and Distribution Piping Systems) [25] and existing pipelines passing through permafrost regions in North America, north-west Siberia, Northeastern China including Trans-Alaska (Alyeska) Pipeline System (TAPS), the Norman Wells pipeline (NWOP), the Nadym-Pur-Taz (NPT) gas production complex, and the China-Russia Crude Oil Pipelines (CRCOPs) [2, 26–28].

The steel grade included X60, X70, and X80. Pipelines with larger diameters and high pressures can increase the gas throughput; thus, pipelines with various pipe diameters were selected. The pipe diameter was from 660 mm to 1422 mm. In pipeline engineering, various design factors are used for regions with different risk levels, so four design factors, i.e., 0.72, 0.6, 0.5, and 0.4, were used, and four pipe wall thicknesses were selected for pipes with various diameters. The burial depth of the pipeline was selected as 1.8 m by the practice in the Arctic region which meets the requirements of design codes and local regulations.

The soil properties can directly influence the soil constraints on the pipe. For the unfrozen soils, the values of peak soil resistant forces per unit length of pipes and yield displacements in the axial, lateral, and vertical directions can be calculated by the equations suggested by the ALA-ASCE guideline. The axial soil parameters were calculated by the backfill soil properties, while the lateral and vertical soil parameters were calculated by site soil properties [29]. In geohazard areas, soft sands are commonly used as backfill soils for pipelines [24].

For frozen soils, the vertical bearing and uplift peak soil resistances are critical for accurate strain prediction. These parameters are often determined by a combination of laboratory testing, field testing, and specialized numerical simulations. A detailed numerical analysis was conducted to determine the vertical bearing peak soil resistance effect on the pipe's structural response. As can be seen from Figure 9, when the vertical bearing peak soil resistance of frozen soils reaches more than 20000 kN/m, the maximum tensile strain of pipe almost does not change with the increase of soil resistance. Taking a conservative approach

Table 1: Sensitivity parameter range of X65, X70, and X80 steel pipelines.

Items	Parameters	Unit	Reference value	Parameter range
Pipe-soil interaction in nonfrost heaving area	Axial peak soil resistance	kN/m	40.5	20~100
	Lateral peak soil resistance	kN/m	318.6	100~2100
	Vertical uplift peak soil resistance	kN/m	52	30~120
	Vertical bearing peak soil resistance	kN/m	1360	1000~5500
Pipe-soil interaction in frost heaving area	Vertical uplift peak soil resistance	kN/m	500	500
	Vertical bearing peak soil resistance	kN/m	20000	20000
Frost heave	Frost heave displacement	m	1	0~1.5
Characteristic of pipe	Diameter of X65 steel pipe	m	0.711	0.66~1.016
	Wall thickness of X65 steel pipe	m	0.0095	0.0079~0.0165
	Diameter of X70 steel pipe	m	0.9144	0.66~1.016
	Wall thickness of X70 steel pipe	m	0.0145	0.01~0.021
	Diameter of X80 steel pipe	m	1.219	0.9144~1.422
	Wall thickness of X80 steel pipe	m	0.0246	0.0184~0.033
Operation	Internal pressure	MPa	10	0~10

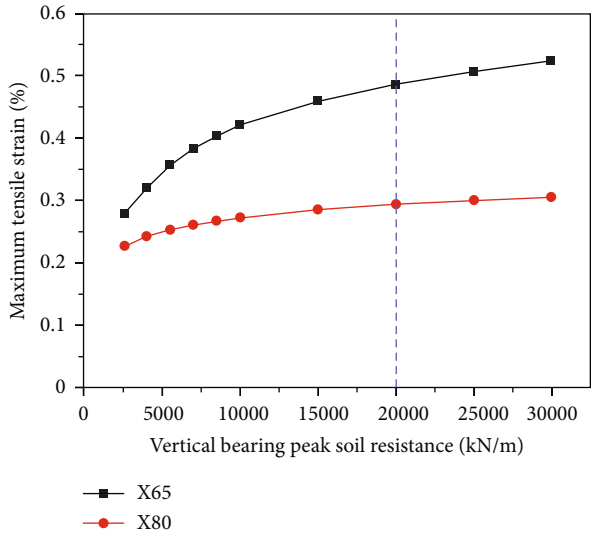

Figure 9: Relationship between maximum tensile strain and vertical bearing peak soil resistance of frozen soils.

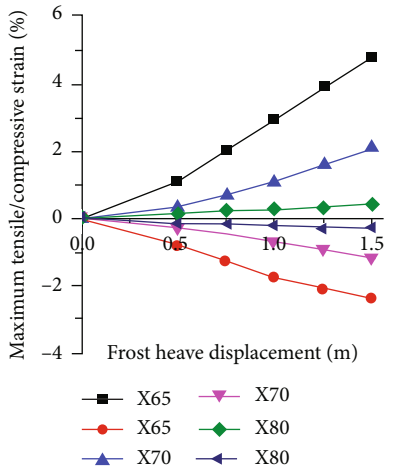

Figure 10: Relationship between maximum tensile and compressive strains and frost heave displacements.

to analysis, for frozen soils, the vertical bearing peak soil resistance was chosen as 20000 kN/m.

The vertical uplift soil resistance mainly depends on soil temperature, pipe displacement rate, and pipe burial depth. The variation curve between vertical uplift soil resistance and pipeline displacement can be described as at the beginning there is a rise in resistance; over a relatively small displacement, the resistance increases to a peak and then decreases from peak to a "residual" resistance. Nixon and Oswell [30] proposed three analytical solutions for peak and residual uplift resistance. One intermediate scale test was carried out by Foriero and Ladanyi [31] at the Caen in France. In addition, there have been several small-scale laboratory tests to measure peak and residual uplift resistance [32, 33]. However, laboratory test data cannot be directly applied to engineering because of two scaling deficiencies: gravity effects and creep effects. The vertical uplift peak soil resistance was initially chosen as 500 kN/m. However, the determination of accurate soil spring resistance is an important work in ongoing research.

The single factor alternative method was used in this systematic analysis. The sensitivity parameters analyzed include soil spring resistance, frost heave displacement, pipeline steel grade, pipeline diameter, wall thickness, and internal pressure.

3.2. Parametric Analysis

3.2.1. Effects of Frost Heave Displacement. The frost heave displacement directly affects the axial strain of the buried pipeline. The pipe was loaded with several displacements from 0.25, 0.5, 0.75, 1.0, 1.25, and 1.5 m to calculate pipeline tensile and compressive strains (Figure 10). The maximum tensile and compressive strains of all steel grade pipes increase with the increase of frost heave displacement. Under the same frost

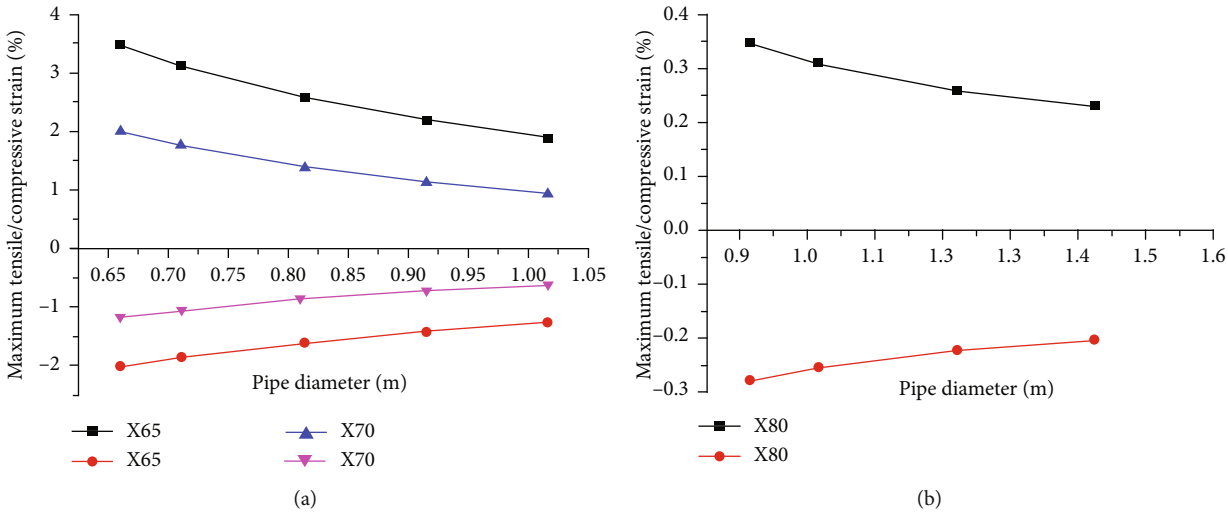

Figure 11: Relationship between maximum tensile and compressive strains and pipe diameter: (a) X65 and X70 steel grade and (b) X80 steel grade.

heave displacement, the larger the steel grade is, the smaller the design strain is, indicating that the high steel grade pipe has a stronger ability to resist deformation.

3.2.2. Effects of Pipe Diameter. The maximum tensile and compressive strains of all steel grade pipes show a decreasing trend with the increase of diameter (Figure 11). As the diameter spans of X65 and X70 steel pipe are different from X80 steel pipe, they are presented separately. The relationship between design strains and pipe diameter is approximately linear, and larger pipe diameter has better resistance to deformation.

3.2.3. Effects of Pipe Wall Thickness. The maximum tensile and compressive strains of all steel grade pipes decrease with the increase of wall thickness (Figure 12). The reason is that larger wall thickness can increase pipe stiffness. The design strain is linearly related to the wall thickness. The pipe with a larger wall thickness has a better ability to resist deformation.

3.2.4. Effects of Pipe Internal Pressure. The internal pressure of the pipe was chosen as 0, 2, 4, 6, 8, and 10 MPa for analysis (Figure 13). For X80 steel pipe, the design strains are almost unchanged under different internal pressures. For X65 and X70 steel pipes, the design strains are also not affected much by internal pressures. Especially under the condition of small internal pressures (≤6 MPa), the design strains are not influenced. This indicates that the internal pressure is not the key influencing factor on the design strain.

3.2.5. Effects of Peak Soil Resistance of Unfrozen Soils. The vertical uplift, vertical bearing, and axial peak soil resistance of unfrozen soils were analyzed (Figure 14). The results show that with the vertical uplift peak soil resistance increasing, the maximum tensile and compressive strains of the X65~X80 steel pipeline maintain a linear increasing trend (Figure 14(a)). The reason is that with the increase of vertical uplift peak soil resistance, the pipe is subjected to a larger bending load which causes larger bending strain and longitudinal strain. When changing the vertical bearing peak soil resistance, the pipeline strains remain unchanged (Figure 14(b)). The reason is that the vertical bearing peak soil resistance of frozen soils is much larger than the one of unfrozen soils. Due to the pipe being mainly affected by bending moment under frost heave displacement, the axial peak soil resistance has little effect on the pipe strain (Figure 14(c)).

3.3. Summary of Influencing Rules. The parametric sensitivity analysis indicates that the frost heave displacement, pipeline diameter, wall thickness, and vertical uplift peak soil resistance of unfrozen soils are sensitive parameters in terms of influence on pipe axial strain. The internal pressure, vertical bearing peak soil resistance, and axial peak soil resistance have little effect on pipe strain. The maximum tensile and compressive strains of all steel grade pipes increase with the increase of frost heave displacement. Under the same frost heave displacement, the larger the steel grade is, the smaller the design strain is, indicating that the high steel grade pipe has a stronger ability to resist deformation. The increase of pipe diameter and wall thickness and the decrease of vertical uplift peak soil resistance of unfrozen soils are more helpful to improve the ability to resist pipeline deformation.

4. Predictions of Pipe Strain Demand

4.1. Establishment of Database. Based on influencing rules of parameters analyzed above, a useful and complete package of nonlinear FEM results contribute to establishing a database for predicting strain demand. The internal pressure, vertical bearing peak soil resistance, and axial peak soil resistance were held constant for all frost heave analysis cases with 10 MPa, 1360 kN/m, and 40.5 kN/m, respectively. Both X65 steel pipe and X70 steel pipe included 5 pipe diameters with 660, 711, 813, 914, and 1016 mm, and X80 steel pipe

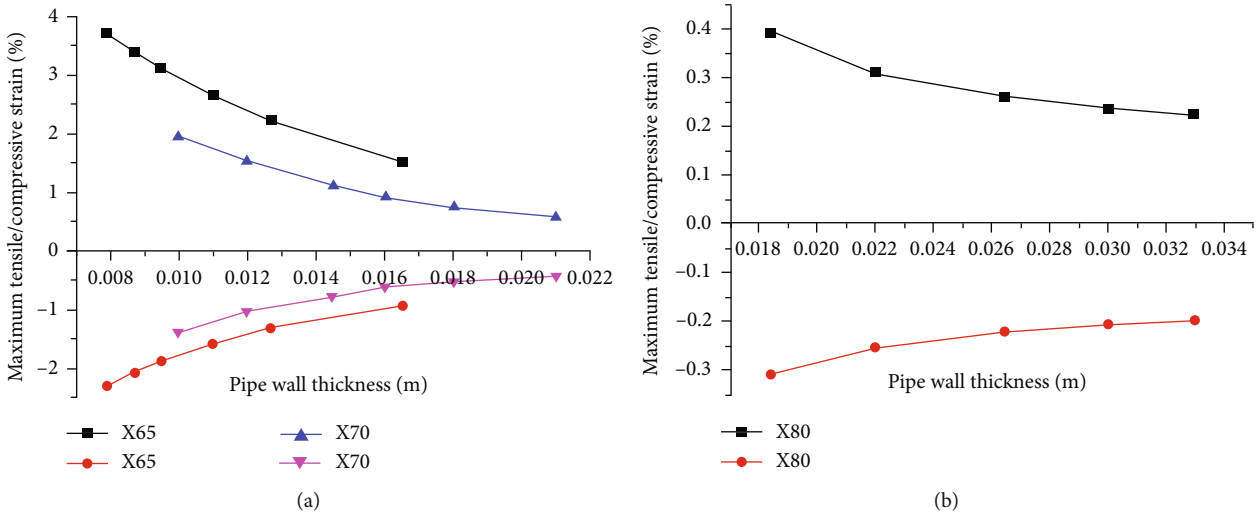

Figure 12: Relationship between maximum tensile and compressive strains and pipe wall thickness: (a) X65 and X70 steel grade and (b) X80 steel grade.

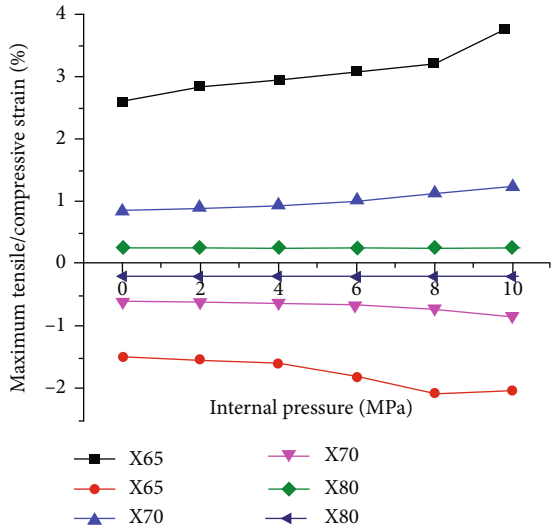

Figure 13: Relationship between maximum tensile and compressive strains and pipe internal pressures.

included 4 pipe diameters with 914, 1067, 1219, and 1422 mm. In addition, 4 wall thicknesses were obtained for each pipe diameter according to the four regional grade design factors required by the code. The frost heave displacements were selected as 0.25, 0.5, 0.75, 1.0, 1.25, and 1.5 m, and the vertical uplift peak soil resistance of unfrozen soils was 30, 40, 50, 60, 70, 80, 90, and 100 kN/m. The total number of calculation examples of X65 steel grade pipeline was $5 \times 4 \times 6 \times 8 \times 1 \times 1 \times 1 = 960$ (among which, the first digit 5 represents the pipe diameter, the second digit 4 for wall thickness, the third digit 6 for the frost heave displacement, the fourth digit 8 for vertical uplift peak soil resistance, and the last three-digit 1 represents the internal pressure, vertical bearing peak soil resistance, and axial peak soil resistance). The total number of calculation examples of X70 steel grade pipeline was $5 \times 4 \times 6 \times 8 \times 1 \times 1 \times 1 = 960$, and the total number of X80 steel grade pipelines was $4 \times 4 \times 6 \times 8 \times 1 \times 1 \times 1 = 768$. The database include a complete package of results based on 2688 individual FEM frost heave simulations.

4.2. Regression Equations. The regression equations of design strain of X65, X70, and X80 steel pipelines under frost heave displacement were fitted utilizing the MATLAB nonlinear fitting toolbox. Taking the X65 steel pipeline, for example, the regression equations for maximum tensile strain and the fitting coefficients obtained are listed as follows. To verify the accuracy of the semiempirical formula, another 38 strain results outside of the FEM results database were selected for comparative analysis (Figure 15). It can be seen that the regression formula is in good agreement with the FEM results with a absolute error of less than 0.4%, indicating high accuracy.

$$\varepsilon = x_1 D^{x_2} t^{x_3} q_u^{x_4} f_u^{x_5} \Delta h^{x_6} \left(x_7 p^2 + x_8 p + x_9\right) X, \tag{2}$$

$$q_u = 2cH + \left(\frac{\phi}{44}\right) \gamma H^2, \tag{3}$$

$$\left\{ \begin{array}{lll} x_1 = 5.5528 \times 10^{-9} & x_2 = -1.4285 & x_3 = -1.1579 \\ x_4 = 0.7104 & x_5 = 0.0318 & x_6 = 1.0528 \\ x_7 = 1 & x_8 = 1.5380 \times 10^{-7} & x_9 = 1.2707 \times 10^{-4} \end{array} \right\}, \tag{4}$$

where X is model deviation, the positional parameter of standard normal distribution μ is 1.0108, scale parameter $\sigma = 0.0590$, D is pipe diameter (m), t is pipe wall thickness (m), p is pipe internal pressure (MPa), $x_1, x_2 \cdots x_9$ is the undetermined coefficient, $\triangle h$ is the frost heave displacement (m), f_u is the axial peak soil resistance (kN/m), q_u is the vertical uplift peak soil resistance (kN/m), c is the characteristic bond strength (Pa), H is the buried depth (m) of the pipe centerline, γ is the effective weight of soil (N/m^3), and ϕ is the angle of internal friction of soil.

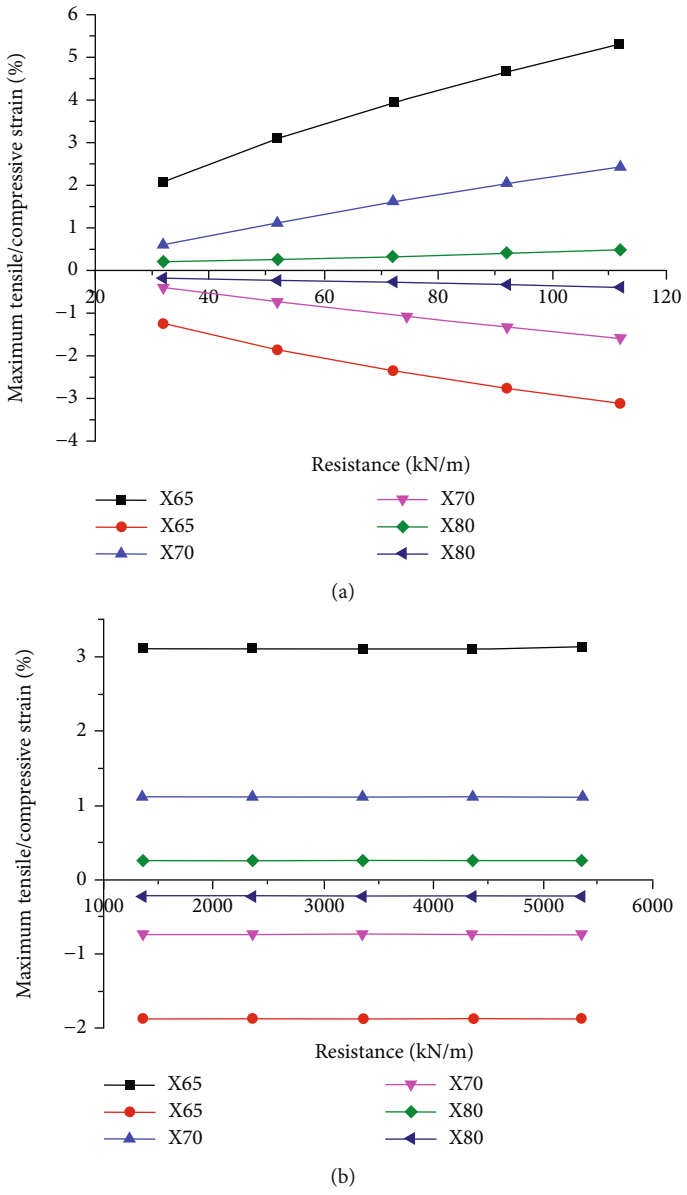

Figure 14: Continued.

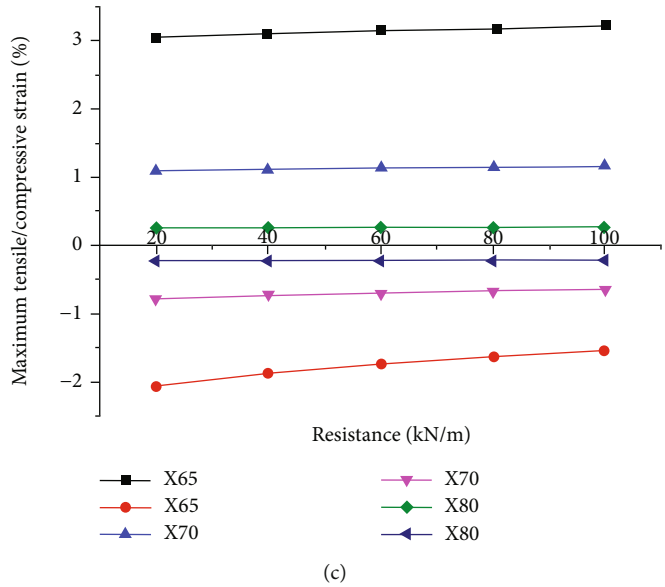

(c)

Figure 14: Relationship between maximum tensile and compressive strains and soil spring resistance of unfrozen soils: (a) vertical uplift peak soil resistance, (b) vertical bearing peak soil resistance, and (c) axial peak soil resistance.

The regression equation for maximum compressive strain is the same as tensile strain and the fitting coefficients obtained are listed as follows. Another 38 strain results outside of the FEM results database were also selected for comparative analysis, and a absolute error of the regression formula is also less than 0.4%.

$$\left\{\begin{array}{lll} x_1 = \text{-}6.0489 \times 10^{-9} & x_2 = -1.0374 & x_3 = -1.2274 \\ x_4 = 0.7030 & x_5 = \text{-}0.1780 & x_6 = 0.5626 \\ x_7 = 1 & x_8 = 2.6157 \times 10^{-6} & x_9 = 1.4475 \times 10^{-4} \end{array}\right\}, \tag{5}$$

where positional parameter of standard normal distribution μ is 1.0092 and scale parameter $\sigma = 0.0815$.

4.3. BPNN. The BPNN was proposed by Rumelhart and McClelland in 1986. It is a multilayer feedforward neural network with three layers (input layer, output layer, and hidden layer). In the error backpropagation, when the errors are not within the range of errors, the errors are backpropagated by adjusting the weights [34, 35]. To predict the design strain of pipelines more quickly, based on the results of FEM, a new BPNN was established to predict pipeline strain under the frost heave displacement.

The frost heave displacement, pipeline diameter, wall thickness, and vertical uplift peak soil resistance were regarded as the four neurons in the input layer and the maximum tensile strain and the maximum compressive strain were regarded as the two neurons in the output layer. The number of hidden layer was determined according to the following empirical formula [16].

$$m = \sqrt{n + l} + \alpha, \tag{6}$$

where m is the number of nodes in the hidden layer, n is the number of nodes in the input layer, l is the number of nodes in the output layer, and a is a constant between 1 and 10. According to multiple iteration trials, the number of nodes in the hidden layer was calculated as $\sqrt{4+2} + 8 = 10$, and the initial network structure was 4 – 10 – 2 (Figure 16).

MATLAB programming was used to create a network. The training data reading, eigenvalue normalization, neural network creation, training parameters setting, model training, and test data reading were realized in turn. Take the X80 steel grade pipeline for example. The total number of the network training samples was 768 groups, of which 70% were used as a training set, 15% as a verification set, and 15% as a test set. After iteration training, the correlation coefficients of the training set, validation set, test set, and overall set were all greater than 0.9999 (Figure 17).

To verify the accuracy of the model, 15 groups of data other than the training samples were substituted into the model for prediction (Figure 18). The results show that the difference between the prediction model and the FEM results is small and the maximum relative error is 10%, indicating that the BPNN is fully trained and the prediction accuracy is good enough in engineering applications. With this trained network, the maximum tensile and compressive strain could be obtained quickly only by inputting four variables such as frost heave displacement, pipe diameter, wall thickness, and vertical uplift peak soil resistance. In addition, the average computing time for one example simulation is 0.08 s, compared with the average time of 3500 s using FEM. This BPNN model could save a lot of time cost and greatly facilitate the strain demand prediction of pipelines under the frost heave displacement.

5. Discussions

The actual strain data of the pipelines in service could be used to validate the accuracy of the new pipeline strain

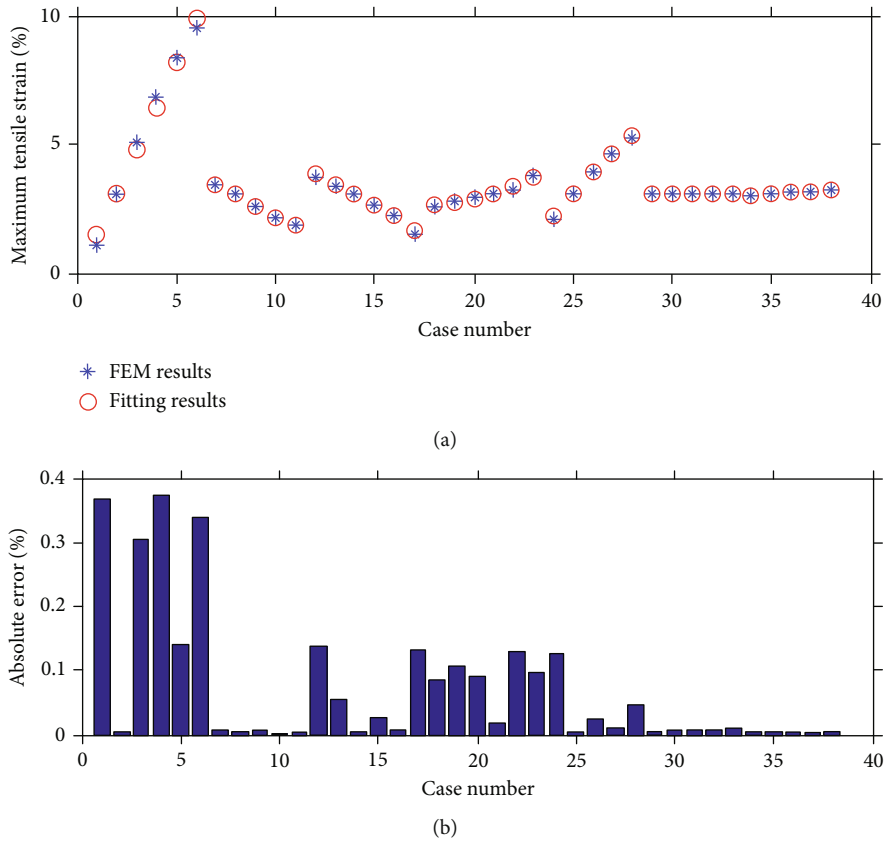

Figure 15: Comparison between semiempirical equation and FEM results for maximum tensile strain: (a) maximum tensile strain and (b) absolute error.

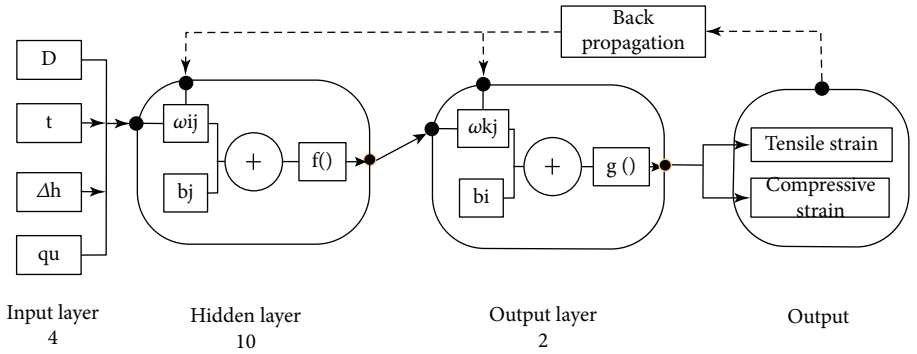

Figure 16: Structure of longitudinal strain prediction model for pipes subjected to frost heave displacement based on BPNN.

prediction methods proposed in the paper. Russia is the only country operating lots of long-distance gas pipelines in permafrost regions. It is advised that the direct monitoring of pipeline axial strain is considered in the design stage of new pipelines. The pipeline strain could be monitored via several technologies. Most notable are in-line inspection (ILI), vibrating wire gauges (VWGs), fiber Bragg grating (FBG), and distributed strain sensing (DSS) with fiber optics [36].

There is another limit state design method called reliability-based design. The load effects and structural resistances are regarded as uncertain quantities characterized probabilistically. For designing a new pipeline, at first, a target reliability level is set and the reliability of the new pipeline should meet the target value. The reliability-based design has received increasingly more attention because the safety criteria are met at a reasonable cost [37]. Arctic pipeline design is evolving towards a reliability-based design with the extreme sensitivity of the environment. In the reliability-based design process, one important work is to develop limit state functions. The research results in this paper including accurate fitting semiempirical equation and BPNN prediction model contribute to formulating limit state functions for the arctic pipeline design. Especially, an enormous number of calculations are needed in reliability-based design.

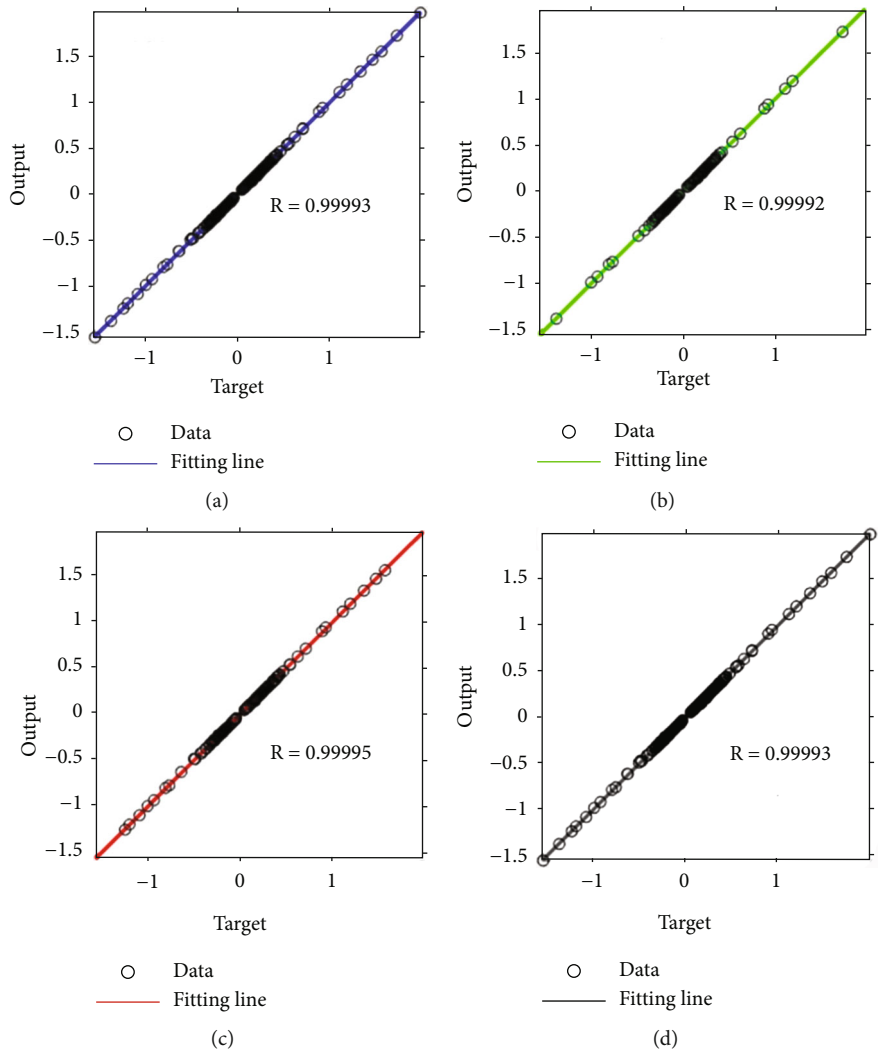

Figure 17: Correlation coefficient R value of BPNN: (a) training set, (b) validation set, (c) test set, and (d) overall set.

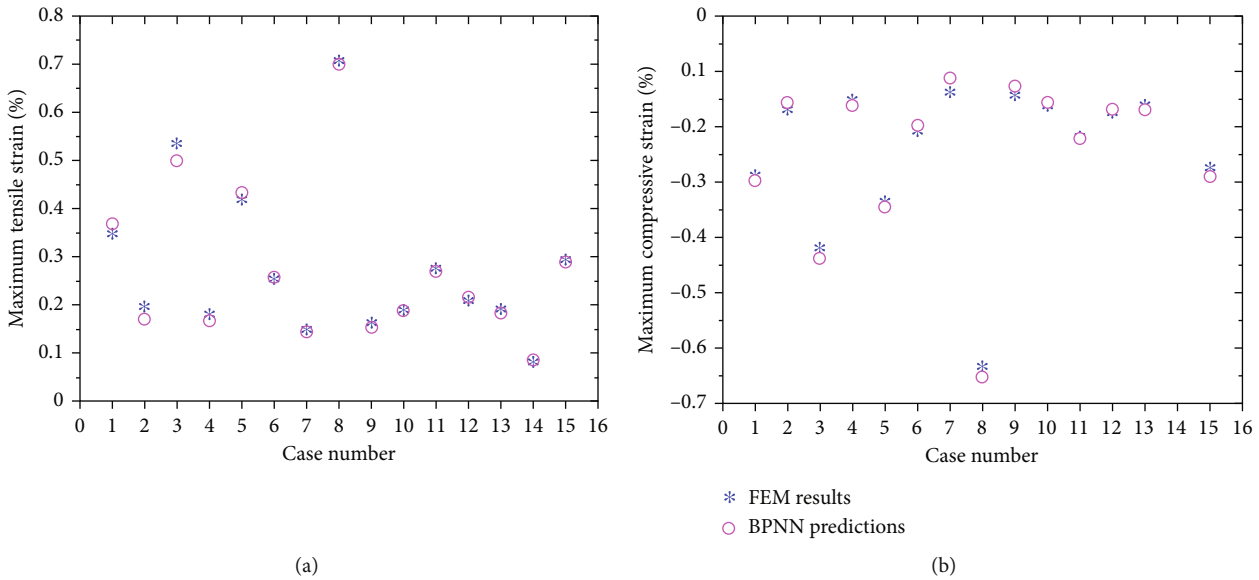

Figure 18: Comparison results of longitudinal strains between the predictions of BPNN and FEM: (a) maximum tensile strain and (b) maximum compressive strain.

The FEM based on numerical methods cannot meet the requirement, because they are very time-consuming [15]. The advantage of the BPNN model is time-saving which is of great practical significance.

6. Conclusions

(1) Two types of nonlinear FEMs: semi-infinite length and finite length models were established and successfully validated with the results of a chilled pipeline experiment carried out at Caen in France. A new customized parametric strain calculation software for the pipeline under frost heave displacement load was also developed, utilizing C# language and object-oriented visual programming techniques.

(2) Based on a complete package of results from the 2688 individual FEM frost heave simulations, the semiempirical equation for predicting strain demand of X65, X70, and X80 steel pipelines under frost heave displacement was presented. The formula was in good agreement with the FEM results with a absolute error of 0.4%, indicating high accuracy.

(3) A BPNN predicting model was also established. Through this trained network, the maximum tensile and compressive strain could be obtained quickly by inputting four variables such as frost heave displacement, pipe diameter, wall thickness, and vertical uplift peak soil resistance. Compared with FEM, the BPNN model was reliable with a relative error of 10% and a lower computing time cost.

Data Availability

The data used to support the findings of this study are available from the corresponding author upon request.

Conflicts of Interest

The authors declare no conflict of interest.

Acknowledgments

This research was funded by the Chinese Academy of Sciences (CAS) Strategic Priority Research Program (Grant No. XDA20100103).

References

[1] X. Z. Li, H. J. Jin, Y. J. Wei, Z. Wen, Y. Li, and X. Y. Li, "Numerical analysis of temperature fields around the buried arctic gas pipe-line in permafrost regions," *Thermal Science*, vol. 25, no. 2 Part A, pp. 869–877, 2021.

[2] A. Brouchkov and G. Griva, "Pipelines on Russian north: review of problems of interaction with permafrost," *Journal of the Japanese Society of Snow and Ice*, vol. 66, no. 2, pp. 241–249, 2004.

[3] H. J. Jin, W. B. Yu, Y. C. Chen, X. F. Gao, F. X. Li, and Z. X. Yao, "(Differential) frost heave and thaw settlement in the engineering design and construction of oil pipeline in permafrost regions: a review," *Journal of Glaciology and Geocryology*, vol. 27, no. 3, pp. 455–464, 2005.

[4] J. M. Konrad and M. Morgenstern, "Frost heave prediction of chilled pipelines buried in unfrozen soils," *Canadian Geotechnical Journal*, vol. 21, no. 1, pp. 100–115, 1984.

[5] G. Y. Li, W. Ma, X. L. Wang et al., "Frost hazards and mitigative measures following operation of Mohe-Daqing line of China-Russia crude oil pipeline," *Rock and Soil Mechanics*, vol. 36, no. 10, pp. 2964–2972, 2015.

[6] K. Koui, Z. Wei, and L. H. Scott, "Frost heave predictions of buried chilled gas pipelines with the effect of permafrost," *Cold Regions Science and Technology*, vol. 53, no. 3, pp. 382–396, 2008.

[7] Y. P. Wu, Y. Sheng, Y. Wang, H. J. Jin, and W. Chen, "Stresses and deformations in a buried oil pipeline subject to differential frost heave in permafrost regions," *Cold Region Science and Technology*, vol. 64, no. 3, pp. 256–261, 2010.

[8] R. X. He and H. J. Jin, "Permafrost and cold-region environmental problems of the oil product pipeline from Golmud to Lhasa on the Qinghai-Tibet Plateau and their mitigation," *Cold Region Science and Technology*, vol. 64, no. 3, pp. 279–288, 2010.

[9] J. F. Nixon and M. Burgess, "Norman Wells pipeline settlement and uplift movements," *Canadian Geotechnical Journal*, vol. 36, no. 1, pp. 119–135, 1999.

[10] J. M. Oswell, "Pipelines in permafrost: geotechnical issues and lessons," *Canadian Geotechnical Journal*, vol. 48, no. 9, pp. 1412–1431, 2011.

[11] A. P. S. Selvadurai and S. B. Shinde, "Frost heave induced mechanics of buried pipelines," *Canadian Geotechnical Journal*, vol. 119, no. 12, pp. 1929–1951, 1993.

[12] Canadian Standard Association (CSA), *Oil and Gas Pipeline Systems; CSA Standard; CSA Z662; Canadian*, Mississauga, ON, Canada, 2003.

[13] B. Liu, X. J. Liu, and H. Zhang, "Strain-based design criteria of pipelines," *Journal of Loss Prevention in Process industries*, vol. 22, no. 6, pp. 884–888, 2009.

[14] M. Burgess and D. Harry, "Norman Wells pipeline permafrost and terrain monitoring: geothermal and geomorphic observations, 1984–1987," *Canadian Geotechnical Journal*, vol. 27, no. 2, pp. 233–244, 1990.

[15] X. B. Liu, Y. F. Chen, H. Zhang et al., "Prediction on the design strain of the X80 steel pipelines across active faults under stress," *Natural Gas Industry*, vol. 34, no. 12, pp. 123–130, 2014.

[16] Q. Zheng, H. Zhang, K. Z. Zhang et al., "Design strain laws and neural network prediction of X80 pipeline under effect of strike-slip fault," *Journal of Safety Science and Technology*, vol. 14, no. 2, pp. 25–32, 2018.

[17] M. Y. Xia, *Strain Based Safety Assessment Method for Pipelines under Thawing Settlement Load, [Ph.D. thesis]*, China University of Petroleum (Beijing), Beijing, China, 2019.

[18] J. Zhou, D. Horsley, and B. Rothwell, "Application of strain-based design for pipelines in permafrost areas," *Proceeding of 2006 international pipeline conference*, 2006, pp. 899–907, Calgary, Alberta, Canada, 2006.

[19] W. Ramberg and W. R. Osgood, "Description of stress-strain curves by three parameters," Technical Note No. 902, National Advisory Committee for Aeronautics, Washington, DC, USA, 1943.

[20] American Society of Civil Engineers, *Guidelines for the Design of Buried Steel Pipe*, American Lifelines Alliance, Reston, VA, USA, 2005.

[21] P. J. Williams, D. W. Riseborough, and M. W. Smith, "The France-Canada joint study of deformation of an experimental pipe line by differential frost heave," *Proceedings of the 2nd International Offshore and Polar Engineering Conference*, 1993, pp. 56–60, San Francisco, CA, USA, 1993.

[22] A. P. S. Selvadurai, J. Hu, and I. Konuk, "Computational modelling of frost heave induced soil-pipeline interaction I: Modelling of frost heave," *Cold Region Science and Technology*, vol. 29, no. 3, pp. 215–228, 1999.

[23] A. P. S. Selvadurai, J. Hu, and I. Konuk, "Computational modelling of frost heave induced soil-pipeline interaction: II. Modelling of experiments at the Caen test facility," *Cold Region Science and Technology*, vol. 29, no. 3, pp. 229–257, 1999.

[24] M. Y. Xia and H. Zhang, "Stress and deformation analysis of buried gas pipelines subjected to buoyancy in liquefaction zones," *Energies*, vol. 11, no. 9, p. 2334, 2018.

[25] American Society of Mechanical Engineers, *Gas Transmission and Distribution Piping Systems; ANSI/ASME2016, B31: 8*, American Society of Mechanical Engineers, New York, NY, USA, 2016.

[26] G. Y. Li, Y. Sheng, H. J. Jin et al., "Development of freezing-thawing processes of foundation soils surrounding the China-Russia Crude Oil Pipeline in the permafrost areas under a warming climate," *Cold Region Science and Technology*, vol. 64, no. 3, pp. 226–234, 2010.

[27] B. J. Seligman, "Long-term variability of pipeline-permafrost interactions in northwest Siberia," *Permafrost and Periglacial Processes*, vol. 11, no. 1, pp. 5–22, 2000.

[28] B. J. Seligman, "Reliability of large-diameter gas pipelines in northern Russia," *Petroleum Economist*, vol. 66, pp. 80–82, 1999.

[29] C. L. Jiang, P. C. Chen, R. Li, and X. Liu, "A multisource monitoring data coupling analysis method for stress states of oil pipelines under permafrost thawing settlement load," *Mathematical Problems in Engineering*, vol. 2020, 15 pages, 2020.

[30] J. F. Nixon and J. M. Oswell, "Analytical solutions for peak and residual uplift resistance of pipelines," *Proceedings of the 63rd Canadian Geotechnical Conference and 6th Canadian Permafrost Conference*, 2010, pp. 12–16, Alta, Calgary, 2010.

[31] A. Foriero and B. Ladanyi, "Pipe uplift resistance in frozen soil and comparison with measurements," *Journal of Cold Regions Engineering*, vol. 8, no. 3, pp. 93–111, 1994.

[32] J. F. Nixon, "Pipe uplift resistance testing in frozen soil," *Proceedings of the 7th International Permafrost Conference*, 1998, pp. 23–27, Yellowknife, NT, USA, 1998.

[33] J. F. Nixon and B. Hazen, "Uplift resistance of pipes in frozen soil," *Proceedings of the 6th International Permafrost Conference*, 1993, pp. 494–499, Beijing, China, 1993.

[34] T. L. Fu and W. Chen, "A hybrid wind speed forecasting method and wind energy resource analysis based on a swarm intelligence optimization algorithm and an artificial intelligence model," *Sustainability*, vol. 10, no. 11, p. 3913, 2018.

[35] G. B. Huang, Q. Y. Zhu, and C. K. Siew, "Extreme learning machine: theory and applications," *Neurocomputing*, vol. 70, no. 1-3, pp. 489–501, 2006.

[36] S. Villalba and J. R. Casas, "Application of optical fiber distributed sensing to health monitoring of concrete structures," *Mechanical Systems & Signal Processing*, vol. 39, no. 1-2, pp. 441–451, 2013.

[37] D. DeGeer and M. Nessim, "Arctic pipeline design considerations," *Proceedings of ASME 2008 27th International Conference on Offshore Mechanics and Arctic Engineering. American Society of Mechanical Engineers Digital Collection*, 2008, pp. 583–590, Estoril,Portugal, 2008.